J. Membrane Biol. 47, 59–76 (1979)

Coupled Transport of Protons and Anions through Lipid Bilayer Membranes Containing a Long-Chain Secondary Amine

John Gutknecht* and Anne Walter

Department of Physiology, Duke University Medical Center,
Durham, North Carolina 27710,
and Duke University Marine Laboratory, Beaufort, North Carolina 28516

Received 25 September 1978; revised 8 December 1979

Summary. Transport of protons and halide ions through planar lipid bilayers made from egg lecithin and a long-chain secondary amine (*n*-lauryl [trialkylmethyl] amine) in *n*-decane was studied. Net proton fluxes were measured with a pH electrode, and halide fluxes were measured with $^{82}Br^-$ and $^{36}Cl^-$. In membranes containing the secondary amine, a large net proton flux was produced either by a Br^- gradient with symmetrical pH or by a pH gradient with symmetrical Br^-, but not by a pH gradient in Br^--free solutions. This H^+ flux was electrically silent (nonconductive), and the H^+ permeability coefficient was $>10^{-3}$ cm sec^{-1} in 0.1 M NaBr. In Br^--free solutions, H^+ selectivity was observed electrically by measuring conductances and zero-current potentials generated by H^+ activity gradients. The permeability coefficient for this ionic (conductive) H^+ flux was about 10^{-5} cm sec^{-1}, several orders of magnitude smaller than the H^+ permeability of the electroneutral pathway. Large electroneutral Br^- exchange fluxes occurred under symmetrical conditions, and the permeability coefficient for Br^- exchange was about 10^{-3} cm sec^{-1} at pH 5. The one-way Br^- flux was inhibited by substituting $SO_4^=$ for Br^- on the "trans" side of the membrane. These results support a "titratable carrier" model in which the secondary amine exists in three forms (C, CH^+ and CHBr). Protons can cross the membrane either as CHBr (nonconductive) or as CH^+ (conductive), whereas Br^- crosses the membrane primarily as CHBr (nonconductive). In addition to these three types of transport, there is also a pH-dependent conductive flux of Br^- which has a permeability coefficient of about 10^{-7} cm sec^{-1} at pH 5. Experiments with lipid monolayers suggest that the pH dependence of this conductive flux is caused by a change in surface potential of about +100 mV between pH 9.5 and 5.0.

Coupled transports of cations and anions occur in a variety of cell and epithelial membranes. These transport processes may be involved in salt absorption (Schultz, 1977), acid secretion (Sachs, Spenney & Lewin, 1978), or electroneutral anion exchange (Jennings, 1976). A lipid bilayer model for the coupled transport of protons and anions was recently described by Gutknecht, Graves and Tosteson (1978). We found that

* *Mailing address and to whom reprint requests should be made:* Duke Marine Laboratory, Beaufort, N.C. 28516.

0022-2631/79/0047-0059/$03.60

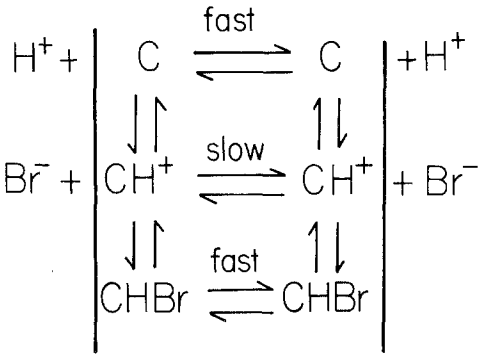

Fig. 1. Model for halide and proton transport through a lipid bilayer membrane containing an organic amine, Amberlite LA-2. C is the free base, CH^+ is the protonated amine, and CHBr is the neutral complex formed with Br^- or other monovalent anions. *See* text for details

anion transport through lipid bilayers containing a long-chain secondary amine, Amberlite LA-2 (*n*-lauryl [trialkylmethyl] amine), shows many similarities to anion transport through red-cell membranes, e.g., high anion selectivity, pH-dependent fluxes, low membrane conductance, and large electroneutral fluxes (Wieth, 1972; Gunn, 1972).

The model developed by Gutknecht *et al.* (1978) which describes the basic features of ion transport through lipid bilayers containing Amberlite LA-2 is shown in Fig. 1. According to this model, halide ions traverse the membrane primarily as the neutral complex, CHBr. This produces large electroneutral (nonconductive) exchange fluxes under symmetrical conditions. Protons cross the membrane via either of two pathways, i.e., nonconductive diffusion via the neutral complex, CHBr, or conductive diffusion via the charged complex, CH^+. The model assumes that the fluxes of H^+ and Br^- via the electroneutral pathway are much faster than the H^+ flux via the conductive pathway.

In our previous study we described the anion exchange properties and some of the electrical properties of lecithin-Amberlite bilayers. In the present study we have tested the model further by measuring electrical properties and net fluxes of H^+ and Br^- under various conditions. Our results generally support the model shown in Fig. 1. However, an additional feature is a pH-dependent halide conductance which may be due to a pH-dependent change in surface potential.

Materials and Methods

Lipid bilayer (optically black) membranes were made by the brush technique of Mueller and Rudin (1969). The experimental membranes were formed from a mixture of

egg lecithin (50 mg/ml) and Amberlite LA-2 (*n*-lauryl [trialkylmethyl] amine) (50 mg/ml) in *n*-decane, which gives lecithin:Amberlite:decane mol ratios of 1:2:82. Control membranes were made from egg lecithin in decane (25–35 mg/ml). Membranes were formed on a 1.4-mm diameter hole in a polyethylene partition which separated two magnetically stirred solutions of 1.2 ml each. The temperature was 22–24 °C.

Net proton fluxes were measured by means of a small combination pH and reference electrode (Fisher Scientific, No. 13-639-92) which was inserted into the rear compartment. In these experiments the front solution was buffered and the rear solution was unbuffered. All solutions were bubbled with nitrogen to remove most of the carbon dioxide. In addition, a nitrogen or argon atmosphere was maintained over the rear compartment and also over the reservoir from which the front compartment was perfused continuously throughout the experiments.

To measure the proton flux, a membrane was formed with unbuffered solution in both compartments. Then the front compartment was perfused continuously with a buffered solution, and the pH in the rear solution was recorded at 1-min intervals. Perfusion was by gravity flow and vacuum aspiration at a rate of 1–2 ml/min. The H^+ activity of the rear solution was plotted against time, and the slope was calculated (*see*, e.g., Figs. 2 and 3). To obtain the net H^+ flux (mol cm^{-2} sec^{-1}), the slope was multiplied by the volume of the rear solution and divided by the surface area of the membrane. The sensitivity of the pH electrode method is about 5×10^{-12} mol cm^{-2} sec^{-1}.

Halide fluxes were usually measured with $^{82}Br^-$ rather than $^{36}Cl^-$, because $^{82}Br^-$ is available in higher specific activities and because the Br^- flux is substantially higher than the Cl^- flux (*see* Table 2). After a stable membrane was formed, $^{82}Br^-$ (as NaBr) was injected into the rear compartment. The rate of appearance of radioactivity in the front compartment was then measured by continuous perfusion (1–2 ml/min) and collection of samples at 3 to 5-min intervals. The perfusate was aspirated from the front compartment and collected in a vacuum trap. The rear compartment was sampled periodically with a microsyringe. The samples were dried in planchets and counted in a low-background counter, and the one-way flux was calculated as described previously (Gutknecht *et al.*, 1978).

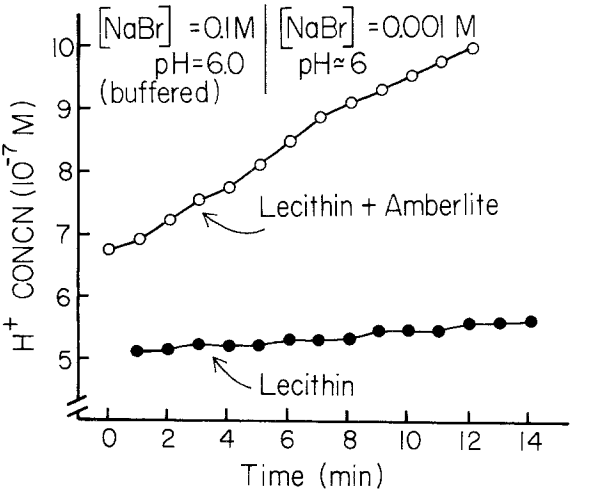

Fig. 2. Net flux of protons generated by a Br^- concentration gradient with approximately symmetrical pH. The front solution contains NaBr (0.1 M) and histidine-$SO_4^=$ buffer (4 mM), pH 6.0. The rear solution contains unbuffered NaBr (0.001 M) and Na_2SO_4 (0.025 M), pH 5.9–6.3

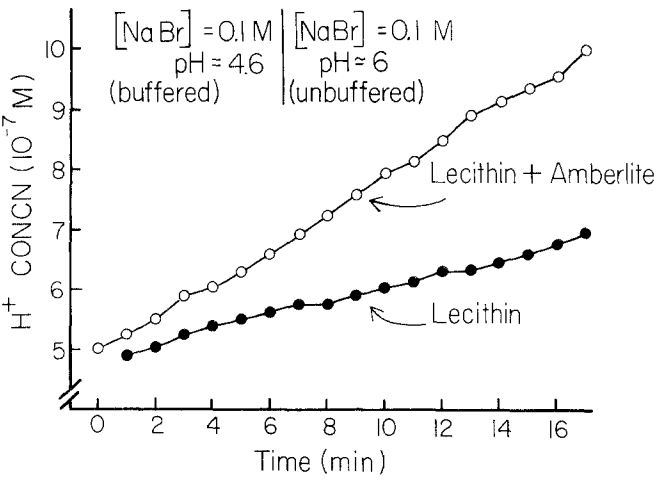

Fig. 3. Net flux of protons generated by a pH gradient with symmetrical Br^- concentrations. Front solution contains NaBr (0.1 M) and Na^+ glutamate buffer (4 mM), pH 4.6. Rear solution contains unbuffered NaBr (0.1 M), pH 6.0–6.3

We calculated the steady-state membrane conductance and membrane current, using Ohm's Law, from the membrane potential produced by applying a known voltage pulse across the membrane in series with a known resistance (voltage divider circuit). The membrane potential was recorded as the potential difference between two calomel-KCl electrodes which made contact with the front and rear solutions, as described by Andreoli, Bangham and Tosteson (1967).

Ion transference numbers were estimated from the zero-current potentials produced by imposing 5- to 10-fold ionic activity gradients across the membrane (*see* Andreoli *et al.*, 1967). From the transference number (t_j) and the total membrane conductance (G_m), we estimated the conductive flux of the ion j by the equation:

$$J_j = \frac{RTt_jG_m}{z_j^2F^2} \tag{1}$$

where R is the gas constant, T is the absolute temperature, z_j is the ionic valence, and F is the Faraday (Hodgkin, 1951). This equation assumes independent ion movement and thus provides an estimate of the rate of simple ionic diffusion through the membrane. This calculated (conductive) flux was subtracted from the observed (tracer) flux in order to estimate the electrically silent component of the observed flux.

The effect of Amberlite on the surface potential of the membrane was estimated by measuring the Volta or surface potentials of lecithin-Amberlite-decane monolayers over the pH range 3.5 to 10. The potential difference between an ionizing electrode (polonium-210) 5 mm above the surface of the monolayer and a Ag/AgCl ground electrode in the aqueous phase was measured with a Keithley 602 electrometer in series with a Hewlett-Packard digital voltmeter. A glass pH electrode and calomel reference electrode were placed in the Teflon trough which contained 20 ml of unbuffered NaBr solution. The solution was stirred continuously with a water-driven magnetic stirrer. The surface of the solution was vacuumed until a steady baseline potential of less than -100 mV was obtained. Then 10 µl of the lipid solution (lecithin:Amberlite:decane, mol ratios 1:2:82, or lecithin:decane, 1:82) were added to the surface with a microsyringe. Adding larger

volumes of lipid solution had no effect on the surface potential. The pH of the aqueous phase was altered by injecting 0.1 M HBr or NaOH. Surface potential and pH were monitored continuously throughout the experiment. At constant pH the surface potential drifted slowly and randomly with time, i.e., less than ± 10 mV/hr.

The surface potential is the sum of the dipole potential, and the potential due to surface charge. Thus,

$$\psi_{\text{surface}} = \psi_{\text{dipole}} + \psi_{\text{charge}}. \tag{2}$$

The surface charge, but not the dipole potential, is dependent on ionic strength of the aqueous phase. The relation between surface charge and ionic strength is given by the Gouy equation (*see* McLaughlin, 1977):

$$\frac{A\sigma}{\sqrt{C}} = \sinh\left(\frac{ze\psi_{\text{charge}}}{2kT}\right) \tag{3}$$

where σ is the surface charge density, C is the concentration of the symmetrical salt, z is the valence of the salt, e is the electronic charge, k is Boltzman's constant, T is the absolute temperature, ψ_{charge} is the potential arising from the surface charge, and $A = (8N\varepsilon_r\varepsilon_0 kT)^{-0.5}$ where N is Avogadro's number, ε_r is the dielectric constant, and ε_0 is the permittivity of free space. If σ is assumed to be independent of salt concentration, then values for ψ_{charge} can be calculated for each concentration by iteratively varying ψ_{dipole} and substituting the value for ψ_{charge} from Eq. (2) into Eq. (3) until the σ's determined at each concentration are equal. Thus, by measuring ψ_{surface} at several ionic strengths we obtained values for ψ_{charge} and ψ_{dipole}.

The estimates of surface charge were also checked by measuring zeta potential. Zeta potentials were calculated from the electrophoretic mobility of lecithin-Amberlite vesicles (mol ratio of vesicle forming mixture was 1:2) and pure lecithin vesicles. We used a cylindrical microelectrophoresis apparatus (Rank Brothers, Cambridge, England) similar to that described by Bangham, Flemans, Heard and Seaman (1958).

Egg lecithin was obtained from Lipid Products (Surrey, England). Amberlite LA-2 was a gift from Rohm and Haas (Philadelphia, Pa.). $^{82}Br^-$ (as NaBr) and ^{36}Cl (as NaCl) were obtained from International Chemical and Nuclear Corp. (Irvine, Calif.).

Amberlite LA-2 is a "technical grade" product which contains a mixture of long-chain secondary amines ranging in mol wt from 353 to 395. The primary source of variation is at the polar end of the molecule where three short hydrocarbon chains contain a total of 11–14 carbons.

The experimental solutions were usually buffered with glutamic acid (pH 3.3–5.1), acetic acid (pH 5.0–5.4) or histidine (pH 5.6–6.5). "Halide-free" solutions were used in some experiments, but these were subject to Cl^- contamination from the calomel electrodes which contained 1 M KCl and had a resistance of about 3×10^4 ohms each. The Cl^- concentration due to leakage from the electrodes was estimated to range from 10^{-7} to 10^{-5} M depending on experimental conditions.

Results

Proton Fluxes

Net proton fluxes were measured under three different conditions, i.e., a Br^- gradient with symmetrical pH, a pH gradient with symmetrical Br^- concentrations, and a pH gradient with Br^--free solutions. For each

Table 1. Net proton fluxes through lipid bilayer membranes

Front solution (buffered)	Rear solution (unbuffered)	A Lecithin + Amberlite (pmol cm^{-2} sec^{-1})	B Lecithin controls (pmol cm^{-2} sec^{-1})	Difference (A–B) (pmol cm^{-2} sec^{-1})
NaBr, 100 mM; Histidine-SO_4, 4 mM; pH 6.0	NaBr, 1 mM; Na_2SO_4, 25 mM; pH 6.0–6.3	$36.9 \pm 2.0(8)$	$6.2 \pm 1.8(6)$	30.7 ± 2.7
NaBr, 100 mM; Na^+ glutamate, 4 mM; pH 4.6	NaBr, 100 mM; pH 6.0–6.4	$35.1 \pm 4.2(7)$	$14.3 \pm 1.1(8)$	20.8 ± 4.3
Na^+ glutamate, 50 mM; pH 4.6	Na_2SO_4, 25 mM; pH 6.0–6.4	$7.4 \pm 1.3(3)$	$10.1 \pm 0.6(3)$	-2.7 ± 1.4

Results are presented in the form: mean ± SE (number of membranes).

condition, net proton fluxes were also measured through egg lecithin-decane bilayers, and these control fluxes were subtracted from the experimental fluxes to obtain the net H^+ flux attributable to the Amberlite. Both the control and experimental flux values include a slow H^+ production due to CO_2 uptake, since the solutions were not completely isolated from the ambient air. The results of two single experiments are shown in Figs. 2 and 3, and the results of all experiments are summarized in Table 1. The data show that in lecithin-Amberlite bilayers a net flux of protons is produced by either a Br^- gradient with symmetrical pH or a pH gradient with symmetrical Br^-, but not by a pH gradient with Br^--free solutions.

During the H^+ flux measurements the membrane voltage was held at zero, but we did not simultaneously measure membrane current due to electrical interference from the pH meter. However, in separate experiments with lecithin-Amberlite bilayers we found that the zero-potential current with a Br^- gradient and symmetrical pH (Table 1, line 1) was about -10^{-7} A cm^{-2} (or about 10^{-12} eq cm^{-2} sec^{-1}), and the zero-current potential was about -40 mV (Br^- diffusion potential). Thus, the net current flow is much too small and in the wrong direction to account for the net H^+ flux, and H^+ must be crossing the membrane in an electrically silent form, presumably as CHBr (*see* Fig. 1). Secondly, with a pH gradient and symmetrical Br^- concentrations (Table 1, line 2) the zero-potential current was not measured because the zero-current potential was not significantly different from zero (<2 mV). With a pH gradient in Br^--free solutions (Table 1, line 3), the zero-potential current

was about 5×10^{-8} A cm^{-2} (ca. 5×10^{-13} eq cm^{-2} sec^{-1}), and the zero-current potential was about +40 mV (H^+ diffusion potential). Although this current may be due to a net H^+ flux, the flux is too small to detect by the pH electrode technique. These electrical data are consistent with our earlier measurements on Amberlite-containing membranes (Gutknecht *et al.*, 1978; Gutknecht & Tosteson, 1970). Additional information on the electrical properties of lecithin-Amberlite bilayers is given below.

A difficulty with these experiments is that the lecithin-Amberlite membranes are rather unstable under most asymmetrical conditions. However, under the conditions shown in Table 1, the membranes thin rapidly (1–2 min) and the pH change over a period of 10–15 min is usually sufficient to provide an accurate estimate of the net H^+ flux (*see* Figs. 2 and 3). Asymmetrical concentrations of H^+ or NaBr had no adverse effect on the stability of lecithin-decane controls.

The net H^+ fluxes shown in Table 1 (lines 1 and 2) are large enough to produce significant gradients in the unstirred layer on the unbuffered side of the membrane. A rough estimate of the H^+ gradient across the unstirred layer can be obtained by Fick's first law, i.e.,

$$J_{HBr} = D_{HBr} \Delta[H^+]/\Delta x^{UL} \tag{4}$$

where J_{HBr} is the net HBr flux through the membrane and unstirred layer (ca. 30 pmol cm^{-2} sec^{-1}), D_{HBr} is the diffusion coefficient of HBr in water (3.1×10^{-5} cm^2 sec^{-1}), $\Delta[H^+]$ is the H^+ gradient across the unstirred layer, and Δx^{UL} is the unstirred layer thickness (ca. 6.5×10^{-3} cm) (Gutknecht & Tosteson, 1973). Solving for $\Delta[H^+]$ yields a value of 7×10^{-6} M, which means that the pH at membrane surface is about 1 pH unit below the pH of the unbuffered solution in the rear compartment. Consequently, a substantial back flux of HBr will occur via the electroneutral pathway, and the net H^+ fluxes shown in Table 1 (lines 1 and 2) will be substantially smaller than the one-way fluxes from front to rear. Furthermore, the net H^+ flux shown in Table 1 (line 1) and in Fig. 2 is actually going against an H^+ gradient of about 10-fold, driven by a Br^- gradient of about 100-fold.

Halide Fluxes

Previously we observed large Br^- exchange fluxes through lecithin-Amberlite bilayers under symmetrical conditions. The electroneutral Br^- flux was proportional to $[H^+]$ over the pH range of about 7 to 4, and

Table 2. Br^- and Cl^- fluxes through lecithin-Amberlite bilayers

Ion	Rear solution	Front solution	One-way flux ($R \rightarrow F$) (10^{-9} mol cm^{-2} sec^{-1})	Membrane permeability coefficient[a] (10^{-4} cm sec^{-1})
Br^-	NaBr, 100 mM; Na acetate, 1 mM; pH 5.0	NaBr, 100 mM; Na acetate, 1 mM; pH 5.0	55 $\pm$3(2)	>5.5[b]
Br^-	NaBr, 100 mM; Na acetate, 2 mM; pH 5.0	Na_2SO_4, 50 mM; Na acetate, 2 mM; pH 5.0	3.2 $\pm$1.2(2)	0.32
Br^-	NaBr, 100 mM; histidine-Br^-, 2 mM; pH 6.0	NaBr, 100 mM; histidine-Br^-, 2 mM; pH 6.0	15 $\pm$7(2)	1.5
Cl^-	NaCl, 100 mM; histidine-Cl^-, 2 mM; pH 6.0	NaCl, 100 mM; histidine-Cl^-, 2 mM; pH 6.0	0.19 $\pm$ 0.10(2)	0.02

[a] The membrane voltage was held at 0 mV, and the permeability coefficient was calculated as the one-way flux divided by the halide concentration in the rear solution.

[b] This permeability coefficient is a lower limit because the Br^- exchange flux is partly limited by diffusion through the unstirred layers at pH 5.

the flux saturated at pH <4. Furthermore, at neutral pH the exchange flux showed nonsaturable kinetics over the range of 1–340 mM NaBr, which was due mainly to the large fraction of nonfunctional Br^- carriers (C) which can be converted by mass action to functional carriers (CH^+) as [Br^-] increases. Table 2 (lines 1 and 3) shows the large Br^- exchange fluxes which occur under symmetrical conditions over the pH range of 5–6. From the membrane conductance at pH 5 (ca. 10^{-5} mhos cm^{-2}) and the Br^- transference number (0.98 ± 0.02) we estimate by Eq. (1) that >99.9% of this exchange flux occurs by an electrically silent mechanism, presumably via the neutral complex, CHBr, as shown in Fig. 1 (Gutknecht *et al.*, 1978).

Table 2 (lines 1 and 2) shows that the one-way Br^- flux is inhibited about 95% by substituting $SO_4^=$ for Br^- on the "trans" side of the membrane, i.e., the side toward which Br^- is moving. Under these conditions the zero-potential current is about 10^{-6} amp cm^{-2} (ca. 10^{-11} eq cm^{-2} sec^{-1}), which is <1% of the residual Br^- flux (Table 2, line 2). Thus, >99% of the residual Br^- flux is electrically neutral, presumably HBr, as shown in Fig. 1. A $Br^- - SO_4^=$ exchange is unlikely because P_{SO_4} is 10,000 times smaller than P_{Br} at pH 5 (Gutknecht *et al.*, 1978). However, we have not excluded the possibility of some Br^--acetate or Br^-

$-Cl^-$ exchange. (The bathing solutions unavoidably contain traces of Cl^- from the calomel-KCl electrodes and also from the pH-reference electrode used during preparation of the experimental solutions.)

If the residual net Br^- flux is largely HBr, as suggested by Fig. 1, then the inhibition caused by "trans" $SO_4^=$ substitution may be primarily due to the development of pH gradients in the unstirred layers. For example, a decreased H^+ concentration in the "cis" unstirred layer will lower the equilibrium concentrations of CH^+ and CHBr on the cis membrane surface and thus decrease the Br^- flux. Alternatively, other steps in the net transport might be rate limiting, e.g., the rate of formation of CH^+ (*see* Gutknecht *et al.*, 1978). Further experiments are obviously necessary, but these will be hindered by the instability of the membranes under these asymmetrical conditions.

Table 2 (lines 3 and 4) also shows that lecithin-Amberlite membranes discriminate between Br^- and Cl^-. The permeability coefficient for Cl^- exchange is only about 1% of that for Br^- exchange under identical conditions. However, the membrane conductance in 0.1 M NaCl at pH 6 is $2\text{–}5 \times 10^{-6}$ mhos cm^{-2}, which is similar to the conductance in 0.1 M NaBr. From Eq. (1), the maximum conductive flux of Cl^- flux is only about 1% of the observed exchange flux. Thus, about 99% of the Cl^- flux is electrically silent and presumably occurs by the same mechanism as the Br^- exchange flux.

Although we have not measured fluxes of other halides, we have measured the one-way Br^- fluxes from 0.1 M NaBr into "trans" solutions containing other Na^+ salts. The relative Br^- fluxes induced by trans anion substitutions were $SCN^- > NO_3^- > Br^- > Cl^- > F^- > SO_4^=$, which corresponds to Eisenman's Sequence I (*see* Wright & Diamond, 1977). The same sequence was obtained for the zero-potential currents, which were measured during the trans anion substitution experiments. These results agree with previous work by Shean and Sollner (1966) and indicate a relatively weak field strength for the anion binding site on Amberlite LA-2.

Electrical Properties of Lecithin-Amberlite Bilayers

The model shown in Fig. 1 indicates that the only charge carrier in lecithin-Amberlite bilayers is the protonated amine (CH^+). If so, it should be possible to demonstrate H^+ selectivity and conductance in lecithin-Amberlite bilayers. In Fig. 4 the zero-current membrane poten-

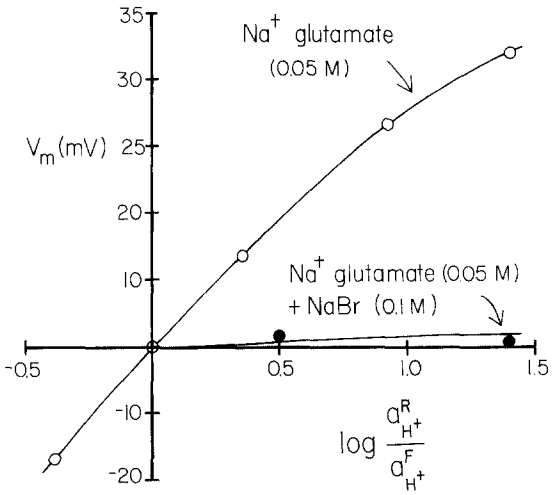

Fig. 4. Zero-current potentials generated by proton activity gradients across lecithin-Amberlite bilayers in the presence and absence of Br^-. Rear solution contains Na^+ glutamate (0.05 M), pH 3.7. Front solution contains Na^+ glutamate (0.05 M), pH 3.3 to 5.1. The membrane potential is that of the front solution with respect to the rear

tial is plotted as a function of the H^+ activity gradient in Br^--free solutions. To generate the curve shown in Fig. 4, the pH of the rear solution was held at 3.7 and the pH of the front solution was varied stepwise from 3.3 to 5.1. The lecithin-Amberlite membranes show good, but not perfect, H^+ selectivity in these Br^--free solutions.

In the Br^--free solutions the only major ions present are glutamate, H^+ and Na^+. If we assume that glutamate is impermeant (and that traces of Cl^- from the electrodes are not important), then the data shown in Fig. 4 yield a H^+ transference number of about 0.9 at pH 3.3 and about 0.6 at pH 5.1. The Na^+ transference number is thus about 0.1 at pH 3.3 and 0.4 at pH 5.1. The pK's of glutamic acid are 2.19 (carboxyl), 4.25 (carboxyl) and 9.67 (amino). Thus, the Na^+ concentration increases from about 5 mM at pH 3.3 to about 44 mM at pH 5.1. This increasing Na^+ and decreasing H^+ concentration probably explains the curve bending away from the voltage axis at high pH.

The lecithin-decane controls showed Na^+ rather than H^+ selectivity under the conditions shown in Fig. 4. For example, the same gradient which produced a 27 mV H^+ diffusion potential in lecithin-Amberlite bilayers produced -6 mV Na^+ diffusion potential in pure lecithin bilayers, which yields a Na^+ transference number of about 0.8 (data not shown).

The membrane conductance of lecithin-Amberlite bilayers in Br^--free sodium glutamate solutions ranged from 1×10^{-7} to 2×10^{-6} mhos cm^{-2} over the pH range of 3.3 to 4.6. This was not significantly higher than the lecithin-decane controls, which ranged from 7×10^{-8} to 1×10^{-6} mhos cm^{-2} over the same pH range. In this series of experiments the conductance of the lecithin-decane controls was rather high compared to the expected value of $<10^{-7}$ mhos cm^{-2}. The reason for this is not known. Nevertheless, in Br^--free solutions the proton conductance induced by Amberlite is $<2 \times 10^{-6}$ mhos cm^{-2}. In 0.1 M NaBr, however, the membrane conductance is much higher, ranging from about 10^{-5} mhos cm^{-2} at pH 5 to almost 10^{-4} mhos cm^{-2} at pH 3 (Gutknecht *et al.*, 1978). Thus, the failure of lecithin-Amberlite bilayers to show H^+ selectivity in the presence of NaBr (Fig. 4, lower curve) is due to the high Br^- conductance at low pH. This dependence of G_m on the Br^- concentration is shown in Fig. 5. At NaBr concentrations above 0.2 M we were unable to obtain thin (optically black) membranes.

Figure 6 shows the current-voltage relation of lecithin-Amberlite bilayers in Br^--free solutions, and Fig. 7 shows $I-V$ curves at three NaBr concentrations. Instability of the membranes prevented us from examining the $I-V$ relations at voltages higher than those shown in Figs. 6 and 7. Nevertheless, the linearity of the $I-V$ curves suggests that

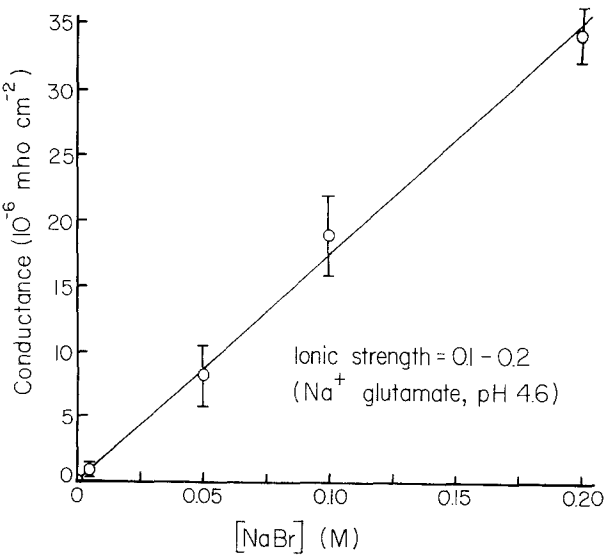

Fig. 5. Steady-state conductance of lecithin-Amberlite membranes as a function of NaBr concentration. Each point shows the mean ± SE of three different membranes

neither carrier gradients within the membrane nor reactions at the membrane surface are limiting the membrane current in either the presence or absence of Br^-. In other words, under all conditions the rate-limiting step appears to be the transmembrane movement of the charged

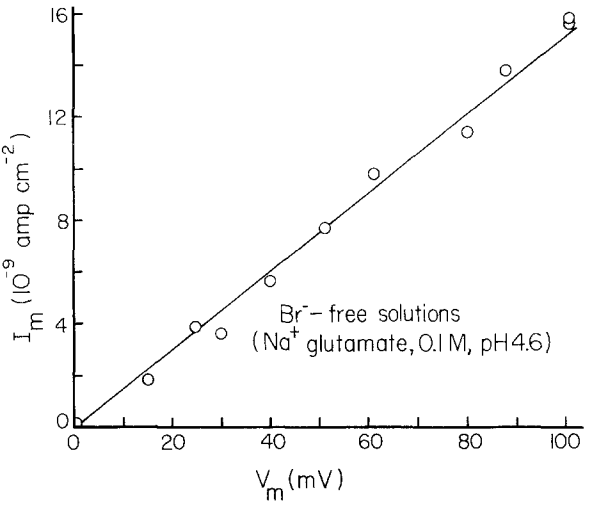

Fig. 6. Current-voltage relation for a lecithin-Amberlite membrane in symmetrical Br^--free solutions (Na^+ glutamate, 0.1 M, pH 4.6)

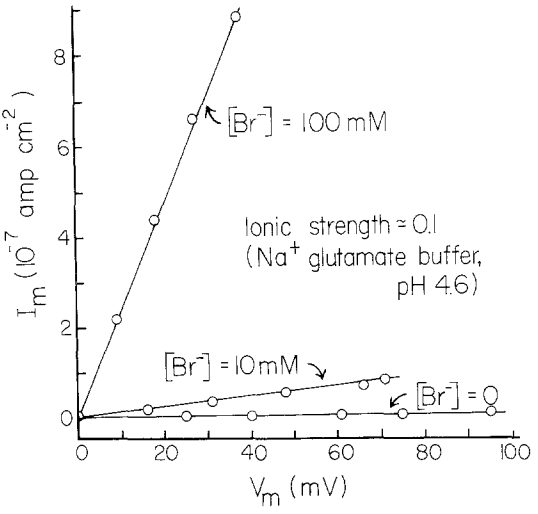

Fig. 7. Current-voltage relations for three different lecithin-Amberlite membranes at three different Br^- concentrations

species, which contradicts an assumption we made previously in attempting to explain the Br^- conductance at low pH (Gutknecht *et al.*, 1978).

The proton selectivity and the linear $I-V$ curve shown in Figs. 4 and 6 are consistent with the model shown in Fig. 1, which suggests a carrier-mediated H^+ transport in which the rate-limiting step is the transmembrane movement of protonated amine, CH^+. However, the data shown in Figs. 5 and 7 are not easily interpreted within the framework of this simple model, which does not provide a mechanism for the Br^- conductance at low pH. In fact, the linearities but differing slopes of the $I-V$ curves in Figs. 6 and 7 suggest that there are two different charge carriers, i.e., CH^+ and Br^-, and that the CH^+ conductance is negligible in the presence of high Br^- concentrations.

Surface Potentials of Lecithin-Amberlite Monolayers

The pH dependence of the Br^- conductance suggests that changes in surface potential of lecithin-Amberlite membranes may be involved in the conductance mechanism. To test this possibility, we measured the surface potentials of monolayers and the zeta potentials of vesicles at several pH values. Figure 8 shows that the surface potential of Amberlite-containing monolayers increases by 114 ± 17 mV (SD) as the pH decreases from 9 to 4, whereas the surface potential of lecithin-decane monolayers is constant over the same pH range. At pH >9, the surface potential of Amberlite-containing monolayers is indistinguishable from that of lecithin-decane controls.

The separate contributions of charge and dipole effects to the surface potential were estimated by measuring surface potentials at different ionic strengths. The shapes of the pH *vs.* $\Delta(\Delta V)$ curves for 10^{-3} M and 1 M NaBr solutions (data not shown) were similar to the upper curve in Fig. 8. However, the maximum changes in voltage were 94 ± 12 mV at 1 M, 114 ± 17 mV at 10^{-1} M, and 190 ± 32 mV at 10^{-3} M NaBr (means $\pm$SD). The best fit of these data to the Gouy equation requires that about 85 mV of the overall potential change be due to dipole effects and the rest (about 29 mV in 10^{-1} NaBr) be due to surface charge effects. This conclusion is consistent with our measurements of zeta potentials, which are sensitive to surface charge only. We obtained a value for lecithin-Amberlite vesicles in 0.1 M NaCl of 26 ± 0.7 mV at pH 3.8, compared to a value of zero for pure lecithin vesicles.

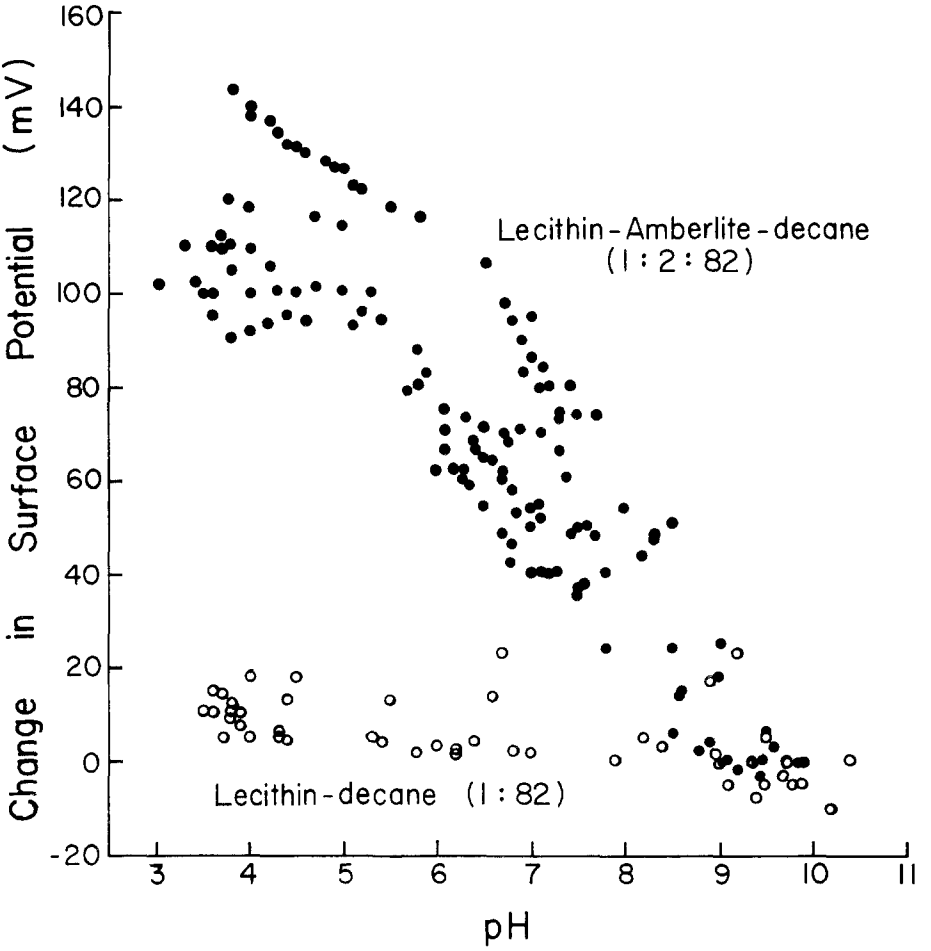

Fig. 8. Changes in surface potentials of monolayers of lecithin-Amberlite-decane (mol ratios 1:2:82) and lecithin-decane (mol ratio 1:82) as a function of pH. Aqueous phase is NaBr (0.1 M) for lecithin-Amberlite monolayers and either NaBr or NaCl (0.1 M) for lecithin controls. Closed circles represent pooled data from six experiments, and open circles represent pooled data from three control experiments

Discussion

Mechanism of H^+ and Br^- Transport

Most of our results support the titratable carrier model shown in Fig. 1, which may be summarized as follows (*see* Table 3). Proton transport occurs by either of two pathways, i.e., CH^+ or CHBr. The CH^+ pathway, observed electrically (Figs. 4 and 5), yields a net proton

Table 3. Summary of H^+ and Br^- permeability coefficients in lecithin-Amberlite bilayers at pH 4–5

Ion flux	Conditions	Method of estimation	Membrane permeability coefficient ($cm\ sec^{-1}$)
H^+ net flux (conductive)	Na^+ glutamate buffer, symmetrical concns.	Electrical	10^{-5}
HBr net flux[a] (nonconductive)	$[H^+]$ gradient with symmetrical $[Br^-]$	pH electrode	$>10^{-3}(H^+)$
HBr net flux[a] (nonconductive)	$[Br^-]$ gradient with symmetrical $[H^+]$	pH electrode	$>10^{-2}(H^+)$
Br^- exchange (nonconductive)	Symmetrical $[Br^-]$	Br^- tracer	10^{-3}
Br^- net flux (conductive)	Symmetrical $[Br^-]$	Electrical	10^{-7}

[a] Net H^+ flux was measured and an equivalent net Br^- flux was assumed. The apparent P_{H^+} in line 3 is higher than the P_{H^+} in line 2 because H^+ is being driven by the Br^- gradient. Both these values are lower limits because of the unstirred layer effects described in the text.

permeability of about 10^{-5} cm sec^{-1} (Table 3, line 1). This permeability is at least 100 times lower than the proton permeability of the CHBr pathway (Table 3, lines 2 and 3), presumably because the neutral complex (CHBr) crosses the membrane much more readily than the charged complex. Furthermore, net fluxes of H^+ and Br^- via the neutral pathway are tightly coupled, so that a net H^+ flux can be driven by either a pH gradient with symmetrical $[Br^-]$ or by a $[Br^-]$ gradient with symmetrical pH, but not by a pH gradient in Br^--free solutions (Table 1, Figs. 2 and 3).

The most conspicuous transport process in lecithin-Amberlite bilayers is the electrically silent Br^- exchange flux, which yields a Br^- permeability coefficient of about 10^{-3} cm sec^{-1} over the pH range of 4–5 (Table 3, line 4). This nonconductive Br^- permeability is about four orders of magnitude larger than the conductive Br^- permeability under identical conditions (Table 3, line 5). Although the conductive H^+ permeability (line 1) is 10^2 times higher than the conductive Br^- permeability (line 5), the total conductance of lecithin-Amberlite bilayers is usually dominated by the Br^- conductance because usually $[Br^-] \gg [H^+]$.

The mechanism of the pH-dependent Br^- conductance is not explained directly by the titratable carrier model in Fig. 1. Some possible explanations include (i) increased permeability to Br^- ions, (ii) existence of an unidentified Br^- complex involving more than one Amberlite molecule, and (iii) Br^- conductance mediated by an unidentified contaminant in Amberlite, which is a "technical grade" product. Of these, the simplest possibility is that the pH-dependent surface potential alters the Br^- ionic conductance according to the relation:

$$G_f = G_0 \exp(-ze\Delta\psi_{surf}/kT) \tag{5}$$

where G_0 and G_f are the initial and final Br^- conductances, z is the valence, e the electronic charge, k the Boltzmann constant, T the absolute temperature, and $\Delta\psi_{surf}$ the change in surface potential (*see* McLaughlin, 1977). Over the pH range of 9 to 4, the surface potential increases by about 114 mV (Fig. 8). Thus, the predicted Br^- conductance will increase by about 96-fold. Insofar as these monolayer results can be applied to bilayers, the observed change in surface potential is probably large enough to explain the pH-dependent Br^- conductance in lecithin-Amberlite-decane membranes (Fig. 5 and Gutknecht *et al.*, 1978). However, a dependence of halide conductance on dipole potentials has not been observed previously in lipid bilayers (*see* McLaughlin, 1977). Thus, additional work is needed to substantiate this hypothesis.

Comparison with Red Cell Anion Transport

In our previous study we listed the similarities between the ionic permeability properties of lecithin-Amberlite bilayers and red cell membranes (Gutknecht *et al.*, 1978). To this list we may now add that the conductive H^+ (or OH^-) permeability is several orders of magnitude higher than the conductive halide permeability at neutral pH (Knauf *et al.*, 1977), and both membranes display cotransport of anions and protons under appropriate conditions (Jennings, 1976).

The phenomena of anion-proton cotransport and nonconductive halide exchange both provide strong evidence for a carrier-mediated transport process (as opposed to a simple channel mechanism) in lecithin-Amberlite bilayers and red cell membranes. However, the carrier mechanisms must differ greatly between these two systems. The red-cell anion carrier apparently functions as a "lock" type carrier in which only a small part of the carrier undergoes a conformational change during

anion transport (Gunn, 1978). Amberlite, on the other hand, probably functions as a classical mobile carrier which moves back and forth through the membrane in a manner similar to that of valinomycin and various other ionophores (*see* Lauger, 1972).

Another difference between Amberlite LA-2 and the red cell anion carrier is the halide permeability sequence. Amberlite, like other weakly basic amines, shows Eisenman's Sequence I, i.e., the Hofmeister series (Shean & Sollner, 1966; Eisenman, 1969; Wright & Diamond, 1977). However, the red-cell anion carrier is "divalent" and the two anion binding sites show very different permeability sequences. The primary binding site for anion exchange is strongly basic ($pK > 11$) (Funder & Wieth, 1976) and shows selectivity sequence *V*, i.e., $Cl^- > Br^- > F^- > I^-$ (Tosteson, 1959). A second binding site may control the net (conductive) anion permeability. This site shows selectivity sequence I (Hunter, 1976) and may be the weakly basic site determined by Funder and Wieth to have a $pK \simeq 6.2$.

The strongly basic nature and high ionization enthalpy of the high pK site led Funder and Wieth to suggest that the site was either a quaternary ammonium or a guanidino group of an arginine residue. Of these two possibilities, the quaternary ammonium seems less likely because in other systems it shows selectivity sequence I rather than V (Wright & Diamond, 1977). A less ambiguous test would be to determine whether the high pK site mediates a halide-hydroxyl exchange or a halide-proton cotransport. Although the net effects of these two processes are similar, the basic mechanisms are different, and a clear distinction is needed for understanding anion transport in any membrane system.

This work was supported in part by National Institutes of Health Grant HL 12157. We thank Dr. Sidney Simon for generous assistance and advice throughout the course of this study.

References

Andreoli, T.E., Bangham, J.A., Tosteson, D.C. 1967. The formation and properties of thin lipid membranes from HK and LK sheep red cell lipids. *J. Gen. Physiol.* **50**:1729

Bangham, A.D., Flemans, R., Heard, D.H., Seaman, G.V.F. 1958. An apparatus for microelectrophoresis of small particles. *Nature (London)* **182**:642

Eisenman, G. 1969. Theory of membrane electrode potentials: An examination of the parameters determining the selectivity of solid and liquid ion exchangers and of neutral ion sequestering molecules. *In:* Ion Selective Electrodes. R.A. Durst, editor. pp. 1–56. National Bureau of Standards, Washington

Funder, J., Wieth, J.O. 1976. Chloride transport in human erythrocytes and ghosts: A quantitative comparison. *J. Physiol. (London)* **262**:679

Gunn, R.B. 1972. A titratable carrier model for both mono- and divalent anion transport in human red blood cells. *In:* Oxygen Affinity of Hemoglobin and Red Cell Acid-Base Status. M.Rørth and P. Astrup, editors. pp. 823–827. Munksgaard, Copenhagen

Gunn, R.B. 1978. Considerations of the titratable carrier model for sulfate transport in human red blood cells. *In:* Membrane Transport Processes. J.F. Hoffman, editor. pp. 61–77. Raven Press, New York

Gutknecht, J., Graves, J.J., Tosteson, D.C. 1978. Electrically silent anion transport through lipid bilayer membranes containing a long-chain secondary amine. *J. Gen. Physiol.* **71**:269

Gutknecht, J., Tosteson, D.C. 1970. Ionic permeability of thin lipid membranes: Effects of *n*-alkyl alcohols, polyvalent cations, and a secondary amine. *J. Gen. Physiol.* **55**:359

Gutknecht, J., Tosteson, D.C. 1973. Diffusion of weak acids across lipid bilayer membranes: Effects of chemical reactions in the unstirred layers. *Science* **182**:1258

Hodgkin, A.L. 1951. The ionic basis of electrical activity in nerve and muscle. *Biol. Rev.* **26**:339

Hunter, M.J. 1976. Human erythrocyte anion permeabilities measured under conditions of net charge transfer. *J. Physiol (London)* **268**:35

Jennings, M.L. 1976. Proton fluxes associated with erythrocyte membrane anion exchange. *J. Membrane Biol.* **28**:187

Knauf, P.A., Fuhrmann, G.F., Rothstein, S., Rothstein, A. 1977. The relationship between anion exchange and net anion flow across the human red blood cell membrane. *J. Gen. Physiol.* **69**:363

Lauger, P. 1972. Carrier-mediated ion transport. *Science* **178**:24

McLaughlin, S. 1977. Electrostatic potentials at membrane-solution interfaces. *Curr. Top. Membr. Transp.* **9**:71

Mueller, P., Rudin, D.O. 1969. Translocators in bimolecular lipid membranes: Their role in dissipative and conservative bioenergy transductions. *Curr. Top. Bioenerg.* **3**:157

Sachs, G., Spenney, J.G., Lewin, M. 1978. H^+ transport: Regulation and mechanism in gastric mucosa and membrane vesicles. *Physiol. Rev.* **58**:106

Schultz, S. 1977. Sodium coupled solute transport by small intestine: A status report. *Am. J. Physiol.* **233**:E249

Shean, G.M., Sollner, K. 1966. Carrier mechanisms in the movement of ions across porous and liquid ion exchanger membranes. *Ann. N.Y. Acad. Sci.* **137**:759

Tosteson, D.C. 1959. Halide transport in red blood cells. *Acta Physiol. Scand.* **46**:19

Wieth, J.O. 1972. The selective ionic permeability of the red cell membrane. *In:* Oxygen Affinity of Hemoglobin and Red Cell Acid-Base Status. M. Rørth and P. Astrup, editors. pp. 265–278. Munksgaard, Copenhagen

Wright, E.M., Diamond, J.M. 1977. Anion selectivity in biological systems. *Physiol. Rev.* **57**:109